Theory of Half-Metal/Superconductor Heterostructures

M. Eschrig,[1] J. Kopu,[1] J. C. Cuevas,[1] and Gerd Schön[1,2]

[1]*Institut für Theoretische Festkörperphysik, Universität Karlsruhe, 76128 Karlsruhe, Germany*
[2]*Forschungszentrum Karlsruhe, Institut für Nanotechnologie, 76021 Karlsruhe, Germany*
(Received 17 June 2002; published 3 April 2003)

We investigate the Josephson coupling between two singlet superconductors separated by a half-metallic magnet. The mechanism behind the coupling is provided by the rotation of the quasiparticle spin in the superconductor during reflection events at the interface with the half metal. Spin rotation induces triplet correlations in the superconductor which, in the presence of surface spin-flip scattering, results in an indirect Josephson effect between the superconductors. We present a theory appropriate for studying this phenomenon and calculate physical properties for a superconductor/half-metal/superconductor heterostructure.

Introduction.—The interplay between superconductivity and spin-polarized materials has potential applications in the emerging field of spin electronics. For this purpose, a high degree of spin polarization of the materials in contact with superconducting regions is desirable. The recently discovered half metals are ideal materials in this respect [1]. In half metals, electronic bands exhibit insulating behavior for one spin direction and metallic behavior for the other. They are thus completely spin-polarized magnets. Half-metallic behavior has been found experimentally in the manganese perovskite $La_{0.7}Sr_{0.3}MnO_3$ [2,3] and in CrO_2 [4]. The perovskite is particularly interesting because of its ability to form high-quality heterostructures with high-T_c cuprate superconductors [5].

The superconducting proximity effect in spin-polarized materials has attracted considerable attention recently in the context of superconductor/ferromagnet heterostructures [6–11]. The singlet pairing amplitude shows oscillations with a wave vector matching the spin splitting of the Fermi wave vectors in the ferromagnet [11,12]. The magnitude of this proximity effect decreases with increasing spin polarization. In the extreme case of a completely spin-polarized material, the singlet proximity effect is absent. Consequently, the Josephson current between two singlet superconductors separated by a half metal is expected to be exactly zero. In this Letter, we show that this is not necessarily the case. We propose a mechanism which leads to a nonvanishing superconductor/half-metal/superconductor (S/HM/S) Josephson effect.

The indirect Josephson effect requires the interplay of two separate interface effects: spin mixing (or spin rotation) and spin-flip scattering. The former, represented by the phase difference θ between waves of opposite spin orientations reflected from a spin-active interface, introduces triplet correlations at the superconducting side of the S/HM boundary. The latter mediates these correlations to the half-metallic side. To illustrate the spin-mixing effect, consider the reflection of two quasi-particles, $|\uparrow\rangle_k$ and $|\downarrow\rangle_k$, from a half-metallic material (which defines the spin quantization axis). The reflected amplitudes for opposite spins differ in phase, $|\uparrow\rangle_{-k} = e^{i\theta/2}|\uparrow\rangle_k$, $|\downarrow\rangle_{-k} = e^{-i\theta/2}|\downarrow\rangle_k$ [13]. In a superconductor, incoming quasiparticles (k) near the interface form pairs with outgoing quasiparticles ($-k$). As $|\uparrow\rangle_k|\downarrow\rangle_{-k} - |\downarrow\rangle_k|\uparrow\rangle_{-k}$ transforms under reflection into $e^{i\theta}|\uparrow\rangle_k|\downarrow\rangle_{-k} - e^{-i\theta}|\downarrow\rangle_k|\uparrow\rangle_{-k}$, pairing states near such interfaces are singlet-triplet mixtures. This property of spin mixing is intrinsic to any spin-active interface. If, additionally, spin-flip scattering is present at the S/HM interface, the resulting triplet amplitudes induce equal-spin pairing correlations in the half metal, leading to an S/HM/S Josephson effect. Spin-flip scattering is expected to be enhanced, e.g., due to local variations of the spin quantization axis [7], or diffusion of magnetic moments. The importance of these processes was pointed out by recent experiments [14].

The indirect proximity effect introduced above can also be relevant for strong ferromagnets. In the conventional description, the dispersions for spin-up and spin-down bands in ferromagnets are assumed to be identical apart from an energy splitting, given by an effective exchange field h [6,7]. The range of the spin-singlet proximity effect is drastically reduced by a strong exchange field. In contrast, no such suppression occurs in the case of the indirect proximity effect.

Theory.—Our treatment is based on the quasiclassical theory of superconductivity [15]. This theory is formulated in terms of Green's functions (propagators) which are matrices in Nambu-Gor'kov particle-hole space and in spin space. The quasiclassical propagator, $\hat{g}(\hat{\mathbf{k}}, \mathbf{R}, \epsilon)$ depends on energy ϵ, position $\mathbf{R}$, and the direction $\hat{\mathbf{k}}$ of the momentum on the Fermi surface. Its particle-hole diagonal and off-diagonal elements are denoted by spin matrices g and f. The quasiclassical propagator satisfies the Eilenberger equation [15]

$$[\epsilon\hat{\tau}_3 - \hat{\Delta}, \hat{g}] + i\mathbf{v}_f \cdot \nabla_{\mathbf{R}}\hat{g} = 0, \tag{1}$$

with the Fermi velocity, $\mathbf{v}_f(\hat{\mathbf{k}})$, and the singlet order

parameter $\hat{\Delta}(\mathbf{R})$. It is essential for our purpose to determine the spatial variation of the order parameter near the interface region in accordance with the triplet correlations, which decay into the superconducting region on the coherence length scale. In order to ensure current conservation in the whole system, we obtain the spatial variation of $\Delta(\mathbf{R})$ self-consistently,

$$\Delta(\mathbf{R}) = \lambda \int_{-\epsilon_c}^{\epsilon_c} \frac{d\epsilon}{2\pi i} \langle f(\hat{\mathbf{k}}, \mathbf{R}, \epsilon) \rangle_{\hat{\mathbf{k}}} \tanh\left(\frac{\epsilon}{2T}\right). \quad (2)$$

The coupling constant λ and the cutoff energy ϵ_c are eliminated in favor of the transition temperature T_c in the usual manner. The quasiclassical Green's functions are normalized according to $\hat{g}^2 = -\pi^2 \hat{1}$ [15].

Boundary conditions.—A standard method to treat boundary conditions for spin-active interfaces is a scattering-matrix formulation [6,16,17]. However, for the present problem, where the number of spin channels on one side of the interface differs from that on the other, it would be necessary to use the formulation by Millis *et al.* [16], which is rather involved. For this reason, we proceed with an alternative but equivalent approach [18]. It allows us to derive explicit quasiclassical boundary conditions in terms of an auxiliary Green's function, $\hat{g}^0$, which solves the boundary condition for an impenetrable interface and is easy to obtain. The impenetrable interface is characterized by two surface scattering matrices, $\hat{S}$ and $\underline{\hat{S}}$, on either side of the interface. The resulting propagators on the two sides are denoted by $\hat{g}^0$ and $\underline{\hat{g}}^0$, respectively.

At the boundary, incoming propagators, $\hat{g}^0_{\mathrm{in}}$, are connected with outgoing ones, $\hat{g}^0_{\mathrm{out}}$, via the surface scattering matrices by $\hat{g}^0_{\mathrm{out}} = \hat{S}\hat{g}^0_{\mathrm{in}}\hat{S}^\dagger$ [13]. Particle conservation requires unitarity, $\hat{S}^\dagger = \hat{S}^{-1}$. We include the transmission processes through the interface via an effective hopping amplitude $\hat{\tau}$ in a *t*-matrix approximation. We assume translational invariance in the plane of the interface. The quasiclassical hopping amplitudes from left to right differ in general for incoming and outgoing quasiparticles. However, the requirement of current conservation leads to relations between these elements as shown in Fig. 1.

The quasiclassical *t*-matrix equations read

$$\hat{t}_{\mathrm{in}} = \hat{\tau}\underline{\hat{g}}^0_{\mathrm{out}}\hat{\tau}^\dagger(\hat{1} + \hat{g}^0_{\mathrm{in}}\hat{t}_{\mathrm{in}}), \qquad \hat{t}_{\mathrm{out}} = \hat{S}\hat{t}_{\mathrm{in}}\hat{S}^\dagger, \quad (3a)$$

$$\underline{\hat{t}}_{\mathrm{out}} = \hat{\tau}^\dagger\hat{g}^0_{\mathrm{in}}\hat{\tau}(\hat{1} + \underline{\hat{g}}^0_{\mathrm{out}}\underline{\hat{t}}_{\mathrm{out}}), \qquad \underline{\hat{t}}_{\mathrm{in}} = \underline{\hat{S}}^\dagger\underline{\hat{t}}_{\mathrm{out}}\underline{\hat{S}}. \quad (3b)$$

On each side of the interface, the *t* matrix describes the modifications of the quasiclassical propagators due to virtual hopping processes to the opposite side. Finally, we express the full propagator in terms of the decoupled solution $\hat{g}^0$, leading to the boundary conditions for incoming and outgoing propagators,

$$\hat{g}_{\mathrm{in}} = \hat{g}^0_{\mathrm{in}} + (\hat{g}^0_{\mathrm{in}} + i\pi\hat{1})\hat{t}_{\mathrm{in}}(\hat{g}^0_{\mathrm{in}} - i\pi\hat{1}), \quad (4a)$$

$$\hat{g}_{\mathrm{out}} = \hat{g}^0_{\mathrm{out}} + (\hat{g}^0_{\mathrm{out}} - i\pi\hat{1})\hat{t}_{\mathrm{out}}(\hat{g}^0_{\mathrm{out}} + i\pi\hat{1}), \quad (4b)$$

and similarly for $\underline{\hat{g}}_{\mathrm{in}}$ and $\underline{\hat{g}}_{\mathrm{out}}$ [19,20]. In the appropriate
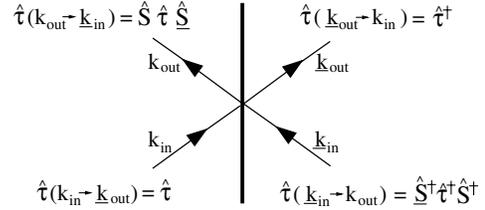
FIG. 1. Scattering geometry illustrating the scattering channels and the corresponding transfer amplitudes for the model discussed in the text.

limiting cases, these boundary conditions reduce to those published previously [21,16,17,22,18].

For reference, we also present the corresponding full scattering matrix which would enter the boundary conditions of Ref. [16]. Without loss of generality, it can be written in the form

$$\hat{\mathbf{S}} = \begin{pmatrix} \hat{S}_{11} & \hat{S}_{12} \\ \hat{S}_{21} & \hat{S}_{22} \end{pmatrix} = \begin{pmatrix} \hat{S} & 0 \\ 0 & \hat{1} \end{pmatrix} \begin{pmatrix} \hat{r} & \hat{d} \\ \hat{d}^\dagger & -\underline{\hat{r}} \end{pmatrix} \begin{pmatrix} \hat{1} & 0 \\ 0 & \underline{\hat{S}} \end{pmatrix}, \quad (5)$$

with the transmission matrix $\hat{d} = (1 + \pi^2\hat{\tau}\hat{\tau}^\dagger)^{-1} \times 2\pi\hat{\tau}$, and the reflection matrices on either side of the interface, $\hat{r} = (1 + \pi^2\hat{\tau}\hat{\tau}^\dagger)^{-1}(1 - \pi^2\hat{\tau}\hat{\tau}^\dagger)$, $\underline{\hat{r}} = (1 + \pi^2\hat{\tau}^\dagger\hat{\tau})^{-1}(1 - \pi^2\hat{\tau}^\dagger\hat{\tau})$.

The particle-hole structures of the surface scattering matrix and the hopping amplitude are $\hat{S} = \mathrm{diag}[S, \tilde{S}]$ and $\hat{\tau} = \mathrm{diag}[\tau, \tilde{S}^\dagger\tau^*\underline{\tilde{S}}^\dagger]$. The above equations are for general spin structures. In the following, τ is a 2×1 spin matrix, S a 2×2 spin matrix, and $\underline{S}$ a spin scalar.

S/HM/S structure.—We study a heterostructure consisting of a half metal, $-L_H < x < L_H$, between two superconductors, $-L < x < -L_H$ and $L_H < x < L$. We investigate the equilibrium supercurrent due to a phase difference ϕ between the superconductors, $\Delta(L) = \Delta(-L)e^{i\phi}$.

As mentioned above, band splitting in the interface region results in a relative spin phase for quasiparticles with spin along the quantization axis of the half metal (for quasiparticles with spin in the perpendicular plane the corresponding effect is a spin rotation around the quantization axis) [13]. This effect can be described by a scattering matrix $\hat{S} = \exp(i\theta\sigma_z/2)\hat{1}$ at the superconducting side of the interface, where θ defines a spin-rotation angle and σ_z denotes the Pauli spin matrix [13,17]. Generally, the value of θ depends on the angle of impact, ψ [13], and can approach values of the order of π for strong band splitting [23]. For definiteness, we present results for $\theta = 0.75\pi\cos\psi$. On the half-metallic side, the scattering matrix has no spin structure, $\underline{\hat{S}} = \hat{1}$.

The *t*-matrix equations are parametrized by the hopping amplitude $\hat{\tau}$ and the scattering matrices $\hat{S}$, $\underline{\hat{S}}$, which are the phenomenological parameters characterizing the interface in our theory. We use $\tau = (1 + S^\dagger)\tau_0 \cos\psi$, where $\tau_0 = (\tau_{\uparrow\uparrow}, \tau_{\downarrow\uparrow})^T$ is determined by the two spin scattering channels from the superconductor to the half-metallic spin-up band. With this choice, the spin rotation during transmission is half of the spin rotation during reflection.

The cosψ factor accounts for the reduced transmission at large impact angles. We present results for $\tau_{\downarrow\uparrow}/\tau_{\uparrow\uparrow} = 0.7$ and 0.1 , $2\pi\tau_{\uparrow\uparrow} = 1.0$, $2L_H = 3\xi_0$ (with the coherence length $\xi_0 = v_f/2\pi T_c$), $L \gg L_H$, and cylindrical Fermi surfaces (calculations using spherical Fermi surfaces lead to similar results). We iterate Eqs. (1) and (2) until self-consistency is achieved, with the boundary conditions (3) and (4) at the two interfaces. All our calculations are in the clean limit.

In Fig. 2, we present the spatial modulation of the singlet order parameter and the triplet pairing correlations for an S/HM/S heterostructure. We compare results for a zero junction ($\phi = 0$) and a π junction ($\phi = \pi$). The spin-rotation effect at the superconducting side of the interface leads to local triplet correlations in the superconductor of the form $f_{\uparrow\downarrow} + f_{\downarrow\uparrow}$. We quantify the triplet pairing correlations by the integral,

$$F_{\text{tripl}}(x) = \int_{-\epsilon_c}^{\epsilon_c} \frac{d\epsilon}{2\pi i} \langle \eta(\hat{\mathbf{k}}) f(\hat{\mathbf{k}}, x, \epsilon) \rangle_{\hat{\mathbf{k}}} \tanh\left(\frac{\epsilon}{2T}\right), \quad (6)$$

where $\eta(\hat{\mathbf{k}})$ projects out the p-wave pairing amplitude, and is equal to the cosine of the angle between $\hat{\mathbf{k}}$ and the surface normal. Spin-flip scattering induces a $F_{\uparrow\uparrow}$ amplitude in the half metal, and leads to both $F_{\uparrow\uparrow}$ and $F_{\downarrow\downarrow}$ amplitudes in the superconductor. The correlations are shown in Fig. 2 for all three spin-triplet channels. Triplet correlations extend into the superconductor up to a few coherence lengths from the interface, leading to a suppression of the singlet order parameter near the interface. We also show schematically the s and p orbitals for a zero junction and a π junction. The alignment of the p orbitals is determined by the direction of the surface normal. As a consequence, the relative sign between the p orbitals is opposite to that of the s orbitals. As will be shown below, this leads to a reversal of the current direction from that expected for a superconductor/normal metal/superconductor junction.

We now turn to the half-metallic region in Fig. 2. The spatial distribution of the proximity-induced $F_{\uparrow\uparrow}$ amplitude shows a sign change at $x = 0$ in the case of zero junction, but not for a π junction. As a result, the π junction is expected to be more stable than the zero junction. Indeed, our numerical calculations show that the π junction corresponds to the free-energy minimum for all temperatures. The equal-spin correlations decay slowly into the half metal, e.g., $F_{\uparrow\uparrow}(x = 0) \propto 1/L_H$ in the π junction. This behavior is similar to that observed in normal metal/superconductor structures.

In Fig. 3, we show the Josephson critical current as a function of temperature. The current density,

$$\mathbf{J} = \int_{-\infty}^{\infty} d\epsilon \langle e\mathbf{v}_f(\hat{\mathbf{k}}) N_\uparrow(\hat{\mathbf{k}}, \epsilon) \rangle_{\hat{\mathbf{k}}} n_f(\epsilon), \quad (7)$$

is expressed in terms of the angle-resolved density of states at the Fermi surface in the half metal, $N_\uparrow = -N_f \text{Im}(g_{\uparrow\uparrow})/\pi$, the electronic charge e, and the Fermi distribution function n_f. In the inset of Fig. 3, we show the current-phase relationship for different temperatures. The current is negative for a positive phase difference ϕ. For each temperature, we determine the critical current from the maximum current magnitude in the current-phase relationship. The critical current has a $(1 - T/T_c)^2$ dependence near T_c. This is a consequence of the fact that the order parameter at the interface varies linearly with

FIG. 2 (color online). Self-consistent order parameter and triplet correlations in an S/HM/S heterostructure for a zero junction and a π junction. The relative signs of the pairing correlations in the s-wave singlet and three p-wave triplet channels are indicated. A zero junction for the singlet order parameter leads to a relative phase difference of π for the triplet correlations, and vice versa. The calculations are for temperature $T = 0.05T_c$, and for $\tau_{\downarrow\uparrow}/\tau_{\uparrow\uparrow} = 0.7$.

FIG. 3 (color online). Critical Josephson current density as a function of temperature for an S/HM/S heterostructure. The two curves are for $\tau_{\downarrow\uparrow}/\tau_{\uparrow\uparrow} = 0.1$ (dashed line) and $\tau_{\downarrow\uparrow}/\tau_{\uparrow\uparrow} = 0.7$ (full line). The inset shows the current-phase relationships for $\tau_{\downarrow\uparrow}/\tau_{\uparrow\uparrow} = 0.7$ for temperatures $T/T_c = 0.05$ (dashed line), 0.2, 0.3, 0.4, and 0.5 (full lines from bottom to top). The unit is the Landau critical current density $J_L = ev_f N_f \Delta_0$, with the zero temperature bulk superconducting gap $\Delta_0 = 1.76T_c$.
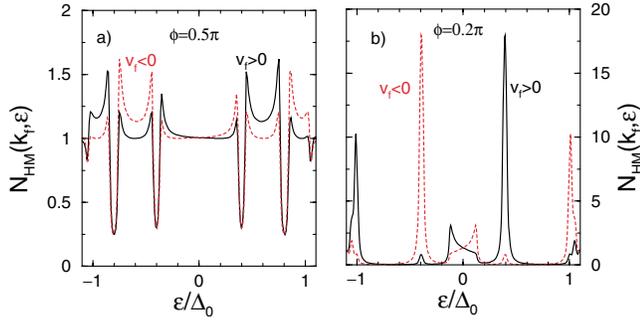
FIG. 4 (color online). Density of states at $T = 0.05 T_c$ for quasiparticles with normal impact at the half-metallic side of the left interface ($x = -L_H$), for (a) spin-flip rate $\tau_{\downarrow\uparrow}/\tau_{\uparrow\uparrow} = 0.1$ and phase difference $\phi = 0.5\pi$, and (b) $\tau_{\downarrow\uparrow}/\tau_{\uparrow\uparrow} = 0.7$ and $\phi = 0.2\pi$. The corresponding Josephson currents are close to the critical values. Shown are both states carrying current in positive (full lines) and negative directions (dashed lines).

$1 - T/T_c$, in contrast to the bulk $(1 - T/T_c)^{1/2}$ behavior. At low temperatures, the critical current passes through a maximum and then decreases again. This anomaly is due to the interplay between current-carrying states, as we proceed to explain.

We discuss the different contributions to the Josephson current coming from the spectral features in the momentum-resolved density of states $N_\uparrow$ in the half metal. The total current through the interface is dominated by quasiparticle trajectories parallel to the surface normal. In Fig. 4, we compare the spectrum of such quasiparticles for incoming and outgoing momenta at the half-metallic side of the left interface. We present results for $\tau_{\downarrow\uparrow}/\tau_{\uparrow\uparrow} = 0.1$ and $\tau_{\downarrow\uparrow}/\tau_{\uparrow\uparrow} = 0.7$. In both cases there is a continuum around the chemical potential ($\epsilon = 0$). On either side of this continuum there is a gap, followed by either additional continuum branches, or by Andreev bound states. The Andreev bound states in Fig. 4(b) are closely related to the surface Andreev states discussed in Refs. [17,23]. According to Eq. (7), the current is obtained by multiplying the curves in Fig. 4 with the Fermi function. At not too low temperatures, the Josephson current is dominated by the negative-energy features below the continuum at the chemical potential. These features carry current in the *negative* direction, explaining the negative sign of the Josephson current for positive phase difference. Below a certain temperature, the corresponding states are fully populated, and the temperature dependence of the Josephson current is dominated by the low-energy continuum around the chemical potential. The current carried by this low-energy band is *positive* and increases with decreasing temperature, leading to the decrease of the magnitude of the critical Josephson current at low temperatures in Fig. 3.

Conclusions.—We have presented a theory for half-metal/superconductor heterostructures and have investigated the Josephson coupling through a half-metallic layer with a thickness of several coherence lengths. The

Josephson coupling is induced by triplet pairing correlations in the superconductor. These triplet correlations are coupled to the singlet superconducting order parameter via a spin-rotation effect, which occurs when quasiparticles in the superconductor are reflected from a spin-polarized medium. We have performed self-consistent numerical calculations for this problem, and found a low-temperature anomaly in the temperature behavior of the critical Josephson current. This anomaly is a robust feature, which is not very sensitive to parameter variations. We discuss the Andreev excitation spectrum in the half-metallic region, and explain the temperature variation of the Josephson current in terms of this spectrum.

[1] W. E. Pickett and J. S. Moodera, Phys. Today **54**, No. 5, 39 (2001).
[2] J.-H. Park *et al.*, Nature (London) **392**, 794 (1998).
[3] R. J. Soulen, Jr. *et al.*, Science **282**, 85 (1998).
[4] Y. Ji *et al.*, Phys. Rev. Lett. **86**, 5585 (2001).
[5] C.-C. Fu, Z. Huang, and N.-C. Yeh, Phys. Rev. B **65**, 224516 (2002).
[6] M. J. M. de Jong and C. W. J. Beenakker, Phys. Rev. Lett. **74**, 1657 (1995); V. I. Fal'ko, A. F. Volkov, and C. J. Lambert, Phys. Rev. B **60**, 15 394 (1999).
[7] F. S. Bergeret, A. F. Volkov, and K. B. Efetov, Phys. Rev. Lett. **86**, 4096 (2001); A. Kadigrobov, R. I. Skekhter, and M. Jonson, Europhys. Lett. **54**, 394 (2001).
[8] M. Giroud *et al.*, Phys. Rev. B **58**, R11872 (1998).
[9] V. T. Petrashov *et al.*, Phys. Rev. Lett. **83**, 3281 (1999).
[10] D. Huertas-Hernando, Yu. V. Nazarov, and W. Belzig, Phys. Rev. Lett. **88**, 047003 (2002).
[11] T. Kontos *et al.*, Phys. Rev. Lett. **89**, 137007 (2002).
[12] A. Buzdin, Phys. Rev. B **62**, 11 377 (2000).
[13] T. Tokuyasu, J. A. Sauls, and D. Rainer, Phys. Rev. B **38**, 8823 (1988).
[14] S. Kreuzer *et al.*, Appl. Phys. Lett. **80**, 4582 (2002).
[15] G. Eilenberger, Z. Phys. **214**, 195 (1968); A. I. Larkin and Y. N. Ovchinnikov, Sov. Phys. JETP **28**, 1200 (1969).
[16] A. Millis, D. Rainer, and J. A. Sauls, Phys. Rev. B **38**, 4504 (1988).
[17] M. Fogelström, Phys. Rev. B **62**, 11812 (2000).
[18] J. C. Cuevas and M. Fogelström, Phys. Rev. B **64**, 104502 (2001).
[19] Current conservation follows from these boundary conditions by verifying $\text{Tr}[\hat{\tau}_3(\hat{g}_{in} + \underline{\hat{g}}_{in} - \hat{g}_{out} - \underline{\hat{g}}_{out})] = 0$.
[20] Equations (3a), (3b), (4a), and (4b) can also be used for Keldysh-Green's functions in nonequilibrium Keldysh formalism. Matrix products then include time convolutions.
[21] A. V. Zaitsev, Sov. Phys. JETP **59**, 1015 (1984); A. L. Shelankov, Sov. Phys. Solid State **26**, 981 (1984).
[22] M. Eschrig, Phys. Rev. B **61**, 9061 (2000); A. Shelankov and M. Ozana, Phys. Rev. B **61**, 7077 (2000).
[23] Yu. S. Barash and I. V. Bobkova, Phys. Rev. B **65**, 144502 (2002).